Available online at www.sciencedirect.com

ScienceDirect

*Mendeleev Commun.*, 2020, **30**, 465–467

Mendeleev Communications

# Nickel-containing nanophases as the carriers of catalytic active sites in the ethylene oligomerization in the presence of systems based on Ni(acac)$_2$ and organoaluminum compounds

**Yuliya Yu. Titova,*[a] Tatyana V. Kon'kova,[a] Boris G. Sukhov[a] and Fedor K. Schmidt[b]**

[a] *A. E. Favorsky Irkutsk Institute of Chemistry, Siberian Branch of Russian Academy of Sciences, 664033 Irkutsk, Russian Federation. E-mail: ytitova60@gmail.com, titova@irioch.irk.ru*

[b] *Department of Chemistry, Irkutsk State University, 664003 Irkutsk, Russian Federation*

DOI: 10.1016/j.mencom.2020.07.019

**The nature and size of particles, formed under conditions of the ethylene oligomerization in the systems based on nickel bis(acetylacetonate) with $Et_2AlCl$ or $Et_2AlCl{\cdot}Cl_2AlEt$ (Al : Ni = = 50 : 1), have been determined using *ex situ* HRTEM, electron diffraction and EDAX in combination with EPR spectroscopy and kinetic studies. It was revealed that the average sizes of Ni-containing particles depend on the nature of cocatalyst and are ~3.5 and ~6 nm for the systems derived from $Et_2AlCl$ and $Et_2AlCl{\cdot}Cl_2AlEt$, respectively. It was shown that these nanoparticles act as the carriers of catalytically active sites during the $C_2H_4$ conversion.**

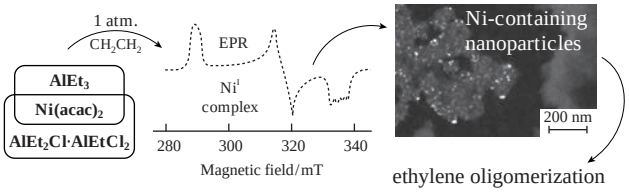


*Keywords*: nanoparticle, nickel, organoaluminum compounds, ethylene, ologomerization, high resolution transmission electron microscopy, electron diffraction, energy dispersive X-ray analysis.

Abundance of natural resources and development of powerful facilities for pyrolysis of oil stock have reduced cost of the lower α-olefins, which consequently gave an impetus to the intensive research on di-, oligo- and polymerization of ethylene, propylene, and butenes. These processes can easily afford butenes, pentenes, hexenes, *etc.*, which are highly sought for the preparation of butadiene, isoprene, higher alcohols, high-octane gasoline, as well as other products of organic synthesis.[1–3]

Multicomponent nickel catalytic systems are active in the conversion of lower α-olefins, *viz.* ethylene, so they continue to attract a great attention of researchers.[4–8] First of all, this is due to their high reactivity under mild conditions and high selectivity towards the products of ethylene di- and trimerization. It is also worthwhile to note that such systems can be employed for the preparation of branched polyethylenes, whereas the reaction selectivity is controlled by modified catalysts bearing 'non-innocent' ligands.[5,7–10] To control all of these phenomena and processes, it is important to comprehend the mechanisms of formation and performance of catalytically active sites.

Different general mechanisms of the formation and performance of catalytically active sites of nickel during ethylene oligomerization/polymerization were reported, where it was assumed that mainly $Ni^{II}$ hydride or alkyl complexes act as the said sites.[11–13] The hypothesis on homogeneous nature of catalysis is considered as dominant,[14,15] although some authors have noted that during the EPR monitoring of alkenes conversion over nickel complex systems, a signal of ferromagnetic resonance appears and grows in the region of $g$ ~2.2 in the EPR spectrum. This signal was assigned to the formation of transition metal particles, the Ni particles in this case.[12,16–19]

Comprehensive studies have been performed using *ex situ* high resolution transmission electron microscopy (HRTEM), electron diffraction and energy dispersive X-ray analysis (EDAX) in combination with EPR and kinetic methods to gain additional information on the phase state of the multicomponent Ziegler catalytic systems, in particular, in order to address the issue on possible presence of nanoscale metal particles and their catalytic activity. In the present work, mixtures of Ni(acac)$_2$ with either $Et_2AlCl$ (diethylaluminum chloride, DEAC) or $Et_2AlCl{\cdot}Cl_2AlEt$ (ethylaluminium sesquichloride, EASC) (Al : Ni = 50 : 1) were selected as the model catalytic systems.†

Mixing of the initial components resulted in Ni(acac)$_2$–DEAC or –EASC based systems,‡ while a triaxially anisotropic signal from the $Ni^I$ complex ($g_1$ = 2.003, $g_2$ = 2.116, and $g_3$ = 2.318) appeared in the corresponding EPR spectra (Figure S1, Online Supplementary Materials). This $Ni^I$ complex possesses a tetragonal structure since $g_\perp < g_\parallel$.[21] Its hyperfine structure (⩾ 4 lines) was observed due to the presence of $^{58}$Ni and $^{35}$Cl atoms in the molecule of the paramagnetic complex ($g_1$ = 2.003). All these data as well as the presence of magnetic moments for $^{35}$Cl ($I$ = 3/2) and $^{27}$Al ($I$ = 5/2) nuclei allowed us to assume that the recorded EPR spectrum can be assigned to the following complex:

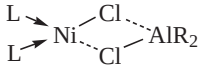


where L is a ligand of the organoaluminium compound and R is Et and/or Cl.

† See Online Supplementary Materials for the catalyst preparation and other experimental details.

‡ Since organoaluminum substances, including DEAC and EASC, are strong reducing agents, they reduce the transition metal complexes to the zero oxidation state upon mixing *via* a series of intermediate steps.[20]

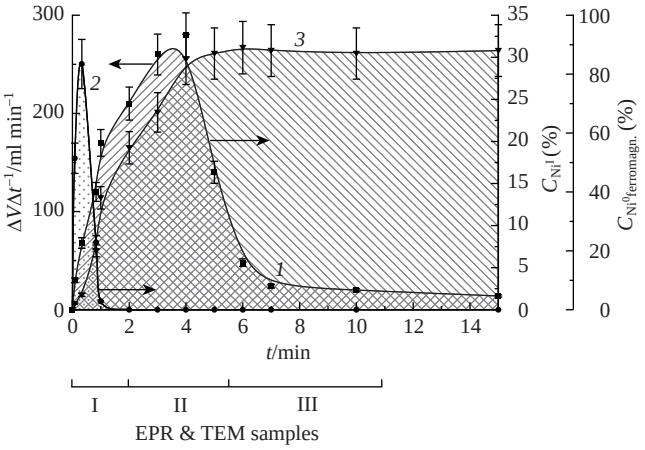


**Figure 1** Time dependences of (*1*) ethylene oligomerization rate, (*2*) calculated $Ni^{I}$ concentration, and (*3*) concentration of Ni in its ferromagnetic state for $Ni(acac)_2$–DEAC system. For clarity, data are presented only for first 15 min of experiment. Time dependences of ethylene oligomerization rate, $Ni^{I}$ and nickel in the ferromagnetic state concentrations for $Ni(acac)_2$–50EASC system are qualitatively similar.

This assumption was also confirmed by a computer simulation of the spectrum (see Figure S1), performed using the EasySpin module for the MatLab software package. The $Ni^{I}$ concentration[§] in the $Ni(acac)_2$–DEAC system varied in the range of 25–30% of the total Ni amount loaded into the reactor (Figure 1). In the case of $Ni(acac)_2$–EASC system, the concentration of $Ni^{I}$ was 55–60%.[19]

When catalytic activity reached its maximum, the $Ni^{I}$ concentration dropped to zero and that of ferromagnetic nickel species has reached 80–90 and 90–95% of the initial nickel complex for the $Ni(acac)_2$–DEAC and $Ni(acac)_2$−EASC systems, respectively (see Figures 1 and S3). TEM samples were taken three times: when the $Ni^{I}$ intensity was maximum (Figure 1, interval I), during the catalyst development (Figure 1, interval II), and after reaching the maximum activity (Figure 1, interval III).[22]

TEM images of samples taken within interval I do not show any particles for both the systems based on $Ni(acac)_2$ and DEAC or EASC [Figures 2(*a*) and 2(*b*), respectively]. The diffraction pattern of both samples is diffuse (see insets in Figure 2), thus evidencing the absence of any crystallinity. Probably, the crystalline structures have not yet reached the size of 0.7 nm (the resolution of the used electron microscope), or thickness of the sample was not sufficient for the TEM detection.[22]

Dark-field TEM images taken within interval II (Figure 3) have demonstrated that for both considered catalytic systems, the samples were coated with a relatively low-contrast (for an electron beam) layer of the different thickness, consisted of organic compounds, inside which higher electron-contrast particles were located. The images recorded using the bright-field TEM method for

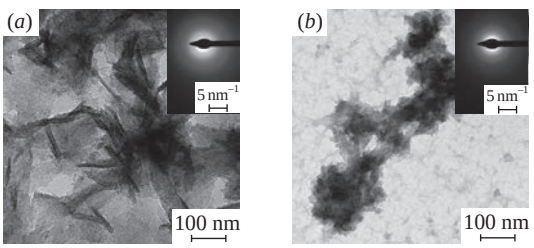


**Figure 2** Bright-field TEM images and electron diffraction (in the inset) of (*a*) $Ni(acac)_2$–DEAC and (*b*) $Ni(acac)_2$–EASC samples taken within first 2 min of the reaction time (interval I in Figure 1).

[§] The $Ni^{I}$ concentration was determined by comparison of the EPR signal area of $Ni^{I}$ complex with that of $Cu(acac)_2$ solution at the given concentration.

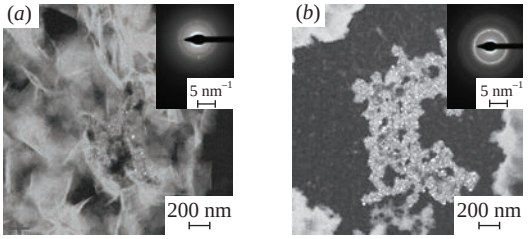


**Figure 3** Dark-field TEM images and electron diffraction (insets) of (*a*) $Ni(acac)_2$–DEAC and (*b*) $Ni(acac)_2$–EASC samples taken within interval II.

$Ni(acac)_2$–DEAC or –EASC derived systems (Figures S4 and S5) showed the high contrast of the particles, indicating their metallic nature. The dark-field HRTEM study[23] has revealed the crystal character of particles (see Figure 3), whose average size was ~3.5 and ~6 nm for $Ni(acac)_2$–DEAC and $Ni(acac)_2$–EASC systems, respectively.

The analysis of atomic series profiles allowed us to suggest that the interplanar distances of 2.08, 2.34, 2.60 and 2.86 Å may correspond to the crystallographic planes of Ni metal or nickel aluminides (## 00-003-1051, 00-004-0850, 00-040-1157, and 00-020-0019) for the $Ni(acac)_2$–DEAC system. The interplanar distances determined by the electron diffraction profiles [see inset in Figure 3(*a*)] were equal to 2.82, 2.07, 1.74 and 1.49 Å, which are also close to the interplanar distances of nickel aluminide (# 00-020-0019).

For the $Ni(acac)_2$–EASC system, the interplanar distances are ~2.14, 2.36, 2.57 and 2.99 Å, which also correspond to the crystallographic planes of Ni metal or nickel aluminides (## 00-003-1051, 00-004-0850, 00-040-1157, and 00-020-0019). The analysis of electron diffraction profiles has revealed the interplanar distances of 2.05, 1.26, 1.21 and 1.08 Å [see inset in Figure 3(*b*)], which are close to the interplanar distances of nickel aluminide (# 00-040-1157).

Nickel-containing nanosize particles scattered in the matrix of organic compounds were also observed in the samples taken within interval III for both systems. No aggregation of the average particle size was observed, while a noticeable agglomeration of the particles was present (Figure 4).

Data acquired by electron diffraction evidence that the particles in samples from interval III for both systems are mainly represented by nickel and nickel aluminides.

The EDAX of organic film indicates the presence of C, H, Al and Cl elements; thus, all the samples are covered with a layer of multicomponent organic matrix. Unfortunately, the thickness of organic matrix did not allow us to acquire any reliable data on the elemental composition of observed particles.

The kinetic data combined with the HRTEM and EPR results unambiguously testify that the appearance and increase of catalytic activity in the $Ni(acac)_2$–DEAC or –EASC (Al : Ni = 50 : 1) systems are due to the presence and intensity of a ferromagnetic resonance signal in the region of $g$ ~2.2. This signal arises due to the formation of nickel-containing nanoclusters, whose size depends on the nature of cocatalyst. The average size of particles almost doubles upon going from DEAC to EASC. Probably,

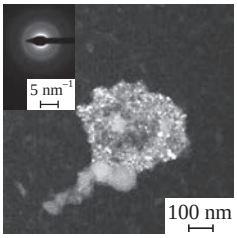


**Figure 4** Dark-field TEM image and electron diffraction (inset) of $Ni(acac)_2$–EASC sample taken within interval III.

nickel-containing nanoparticles act as a carrier or support for the catalytically active sites containing $Ni^{II}$–H or $Ni^{II}$–C moieties.

Similarly to the previously proposed model of nickel nanoparticles generated *via* the reaction of $Ni(acac)_2$ with $AlEt_3$,[19] it can be assumed that an excess of either DEAC or EASC cocatalyst (Al : Ni = 50 : 1) is involved in the formation of a stabilizing shell. Moreover, since nickel-containing nanoparticles possess a weak Lewis acidity,[24] some of the aluminum-containing compounds can be bound on the surface of particles according to the acid–base interaction mechanism.

Thus, taking into account a common opinion about homogeneous nature of such systems and given that multicomponent catalytic systems including those based on nickel compounds are widely used in industry,[2] our findings can lead to revision of such quantitative parameters as TOF and TON for such multicomponent systems and open up new routes to the targeted synthesis of highly efficient catalysts for ethylene oligomerization. It should also be mentioned that the presented results additionally confirm that $Ni^{I}$ complexes, which are detected in the described systems immediately after mixing the components, do not directly participate in oligomerization processes. It has also been shown for the first time that these $Ni^{I}$ complexes are involved in the formation of nanosized nickel-containing particles acting as carriers of catalytic activity.

Further studies of these nanoparticles as well as the mechanistic investigations of their formation and performance in the processes of lower alkenes transformation are underway in our laboratory.

In conclusion, we have found that the catalytic activity of multicomponent systems $Ni(acac)_2$–DEAC or –EASC (Al : Ni = 50 : 1) in the processes of ethylene oligomerization is due to the formation of nanosized nickel-containing particles that act as carriers of catalytically active sites bearing $Ni^{II}$–H or $Ni^{II}$–C fragments. It is shown that both average size of nickel-containing particles and the catalytic activity of the above systems depend on the nature of the cocatalyst. The probable composition of the nanosized nickel-containing particles is established. It is proved that the $Ni^{I}$ complexes, which are formed at the intermediate stages of the interaction of the initial components, participate in the formation of nanosized nickel-containing particles, but are not directly involved in the ethylene oligomerization.

This work was performed within the framework of the State Contract (no. AAAA-A19-119022690046-4) of the Program of Fundamental Research. The TEM studies were carried out using the equipment of Baikal Nanotechnology Center (National Research Irkutsk State Technical University). The authors are grateful to the Baikal Analytical Center for Collective Uses of the SB RAS.

*Online Supplementary Materials*

Supplementary data associated with this article can be found in the online version at doi: 10.1016/j.mencom.2020.07.019.

## References

1 Y. Kissin, *Alkene Polymerization Reactions with Transition Metal Catalysts*, ed. G. Centi, Elsevier, Amsterdam, 2008.
2 W. Keim, *Angew. Chem., Int. Ed.*, 2013, **52**, 12492.
3 C. H. Bartolomew and R. J. Farrauto, *Fundamentals of Industrial Catalytic Processes*, 2nd edn., John Wiley & Sons, Inc., Hoboken, NJ, 2005.
4 *Modern Organonickel Chemistry*, ed. Y. Tamaru, Wiley-VCH, 2005.
5 F. Speiser, P. Braunstein and L. Saussine, *Acc. Chem. Res.*, 2005, **38**, 784.
6 V. P. Ananikov, *ACS Catal.*, 2015, **5**, 1964.
7 A. A. Antonov, N. V Semikolenova, E. P. Talsi and K. P. Bryliakov, *J. Organomet. Chem.*, 2019, **884**, 55.
8 C. Huang, V. A. Zakharov, N. V Semikolenova, M. A. Matsko, Q. Mahmood, E. P. Talsi and W. H. Sun, *J. Catal.*, 2019, **372**, 103.
9 K. P. Butin, E. K. Beloglazkina and N. V. Zyk, *Russ. Chem. Rev.*, 2005, **74**, 531 (*Usp. Khim.*, 2005, **74**, 585).
10 L. A. Berben, B. de Bruin and A. F. Heyduk, *Chem. Commun.*, 2015, **51**, 1553.
11 A. Finiels, F. Fajula and V. Hulea, *Catal. Sci. Technol.*, 2014, **4**, 2412.
12 Yu. Yu. Titova, L. B. Belykh and F. K. Schmidt, *Kinet. Catal.*, 2016, **57**, 388 (*Kinet. Katal.*, 2016, **57**, 392).
13 J. Wang, L. Wang, H. Yu, R. U. Khan, M. Haroon, Zain-ul-Abdin, X. Xia and R. U. Khan, *Eur. J. Inorg. Chem.*, 2018, **13**, 1450.
14 *The Handbook of Homogeneous Hydrogenation*, ed. J. G. de Vries, Wiley-VCH, Weinheim, 2007.
15 O. S. Soficheva, G. E. Bekmukhamedov, A. B. Dobrynin, J. W. Heinicke, O. G. Sinyashin and D. G. Yakhvarov, *Mendeleev Commun.*, 2019, **29**, 575.
16 V. S. Tkach, F. K. Schmidt, V. V. Saraev and A. V. Kalabina, *Kinet. Katal.*, 1974, **15**, 617 (in Russian).
17 M. M. Selim and I. H. Abd El-Maksoud, *Microporous Mesoporous Mater.*, 2005, **85**, 273.
18 A. Brückner, U. Bentrup, H. Zanthoff and D. Maschmeyer, *J. Catal.*, 2009, **266**, 120.
19 Yu. Yu. Titova and F. K. Schmidt, *Kinet. Catal.*, 2017, **58**, 749 (*Kinet. Katal.*, 2017, **58**, 735).
20 T. Mole and E. A. Jeffery, *Organoaluminium Compounds*, Elsevier, New York, 1972.
21 *Comprehensive Coordination Chemistry*, eds. G. Wilkinson, R. D. Gillard and J. A. McCleverty, Pergamon Press, Oxford, 1987.
22 J. M. Zuo and J. C. H. Spence, *Advanced Transmission Electron Microscopy. Imaging and Diffraction in Nanoscience*, Springer, New York, 2017.
23 V. I. Bukhtiyarov, V. I. Zaikovskii, A. S. Kashin and V. P. Ananikov, *Russ. Chem. Rev.*, 2016, **85**, 1198.
24 K.-R. Pörschke, W. Kleimann, Y.-H. Tsay, C. Krüger and G. Wilke, *Chem. Ber.*, 1990, **123**, 1267.

*Received: 27th January 2020; Com. 20/6115*